# Climate change is rapidly deteriorating the climatic signal in Svalbard glaciers

Andrea Spolaor[1,2], Federico Scoto[3,2], Catherine Larose[4], Elena Barbaro[1,2], Francois Burgay[5,2], Mats P. Bjorkman[6], David Cappelletti[7], Federico Dallo[2], Fabrizio de Blasi[1,2], Dmitry Divine[8], Giuliano Dreossi[1,2], Jacopo Gabrieli[1,2], Elisabeth Isaksson[8], Jack Kohler[8], Tonu Martma[9], Louise S. Schmidt[10], Thomas V. Schuler[10], Barbara Stenni[2], Clara Turetta[1,2], Bartłomiej Luks[11], Mathieu Casado[12] and Jean-Charles Gallet[8].

[1]CNR-Institute of Polar Science (ISP), Campus Scientifico, Via Torino 155, 30172, Venice-Mestre, Italy.
[2]Department of Environmental Sciences, Informatics and Statistics, Ca' Foscari University, Venice, Italy
[3]Institute of Atmospheric Sciences and Climate, ISAC-CNR. Campus Ecotekne, 73100 Lecce, Italy
[4]Environmental Microbial Genomics, Laboratoire Ampère, CNRS, University of Lyon, France
[5]Paul Scherrer Institute, Laboratory of Environmental Chemistry (LUC), 5232 Villigen PSI, Switzerland
[6]University of Gothenburg, Department of Earth Sciences, Box 460, 40530 Göteborg, Sweden
[7]Dipartimento di Chimica, Biologia e Biotecnologie, Università degli Studi di Perugia, 06123 Perugia, Italy
[8]Norwegian Polar Institute, Tromsø NO-9296, Norway
[9]Department of Geology, Tallinn University of Technology, Ehitajate tee 5, 19086 Tallinn, Estonia
[10]University of Oslo, Department of Geosciences, Oslo, Norway
[11]Institute of Geophysics, Polish Academy of Sciences, Księcia Janusza 64, 01-452 Warsaw, Poland
[12]Laboratoire des Sciences du Climat et de l'Environnement, CEA–CNRS–UVSQ–Paris-Saclay–IPSL, Gif-sur-Yvette, France

Corresponding author: andrea.spolaor@cnr.it

**Abstract**

The Svalbard archipelago is particularly sensitive to climate change due to the relatively low altitude of its main ice fields and its geographical location in the higher North Atlantic, where the effect of the Arctic Amplification is more significant. The largest temperature increases have been observed during winter, but increasing summer temperatures, above the melting point, have led to increased glacier melt. Here, we evaluate the impact of this increased melt on the preservation of the oxygen isotope signal ($\delta^{18}O$) in firn records. $\delta^{18}O$ is commonly used as proxy for past atmospheric temperature reconstructions and, when preserved, it is a crucial parameter to date and align ice cores. By comparing four different firn cores collected in 2012, 2015, 2017 and 2019 at the top of the Holtedahlfonna ice field (1100 m. a.s.l.), we show a progressive deterioration of the isotope signal and we link its degradation to the increased occurrence and intensity of melt events. Although the $\delta^{18}O$ signal still reflects the interannual temperature trend, more frequent melting events may in the future affect the interpretation of the isotopic signal, compromising the use of Svalbard ice cores. Our findings highlight the impact and the speed at which Arctic Amplification is affecting Svalbard's cryosphere.

## Introduction

Arctic regions are undergoing faster warming than the global average, due to the so-called "Arctic Amplification" (Dahlke et al., 2020). Arctic Amplification is caused by various feedback processes in the atmosphere-ocean-ice system and significantly affects the Arctic North Atlantic region. Arctic warming is not seasonally uniform and has the largest impact in the winter months and close to the surface (Rantanen et al., 2022a; Dahlke and Maturilli, 2017). Furthermore, it is not evenly distributed across the Arctic; the largest warming rates are over the Barents/Kara Seas, where autumn and winter sea-ice retreat is the most pronounced (Lind et al., 2018; Isaksen et al., 2022, 2016). However, even at tropospheric levels, there is a significant warming signal in recent decades that peaks in the Svalbard region, and more generally, in the North Atlantic sector of the Arctic (Dahlke and Maturilli, 2017). Rates there are up to four times the global average since 1979 (Rantanen et al., 2022b).

Glaciers and ice caps in the Svalbard archipelago cover an area of ~34,000 $km^2$, representing about 6% of the world's glacier area outside the Greenland and Antarctic ice sheets. Svalbard glaciers contain 7740 ± 1940 $km^3$ (or Gigaton; Gt) of ice, sufficient to raise global sea level by 1.7 ± 0.5 cm if totally melted (Schuler et al., 2020; Geyman et al., 2022; van Pelt et al., 2019). As a result of both Arctic Amplification and their peculiar position at the edge of Arctic sea ice retreat, they are experiencing among the fastest warming on Earth (Noël et al., 2020).

Ongoing climate trends also affect the state of the seasonal snowpack in Svalbard (Østby et al., 2017; van Pelt et al., 2016), with the numbers of days with snow-cover on the ground in Longyearbyen decreasing from 253 (1976-1997) to 219 (2006-2018) (data from Monitoring of Svalbard and Jan Mayen, mosj.no). The change in the Svalbard climate also has strong repercussions for the entire environment of the archipelago, leading to an increase in frequency of Rain on Snow (RoS) events (Wickström et al., 2020; Salzano et al., 2023) which lead to pervasive ice layers(Sobota et al., 2020) covering the ground, limiting access to food for reindeers (Peeters et al., 2019). It has also led to a reduction in sea ice that is limiting and changing the hunting area of polar bears. These changes over time might be captured in ice core records. Ice cores, in fact, are commonly used to derive information about past climate conditions and atmospheric composition, including traces of natural events such as volcanic eruptions (Sigl et al., 2014), anthropogenic contamination(Vecchiato et al., 2020)and past temperature variability (Wolff et al., 2010), revealing that abrupt climate changes have repeatedly occurred over the last ice age. For example, during the so-called Dansgaard-Oeschger events, temperatures rose by about 5°C within centuries (Boers, 2018). However, even during these natural abrupt events, a complete transition from stadial (glacial) to interstadial (warm) conditions took about a century (Scoto et al., 2022; Steffensen et al., 2008). Current temperature rise in Svalbard is much faster than the one observed during the D-O events, with annual mean surface air temperature increasing in average by $+1.3\ \mathrm{K} \pm 0.7\ \mathrm{K}$ per decade, and winter mean temperature increasing by $+3.1 \pm 2.4$ K per decade (Dahlke et al., 2020; Maturilli et al., 2013).

Snowmelt and water percolation at the sampling site can move the chemical constituents across the layers (Spolaor et al., 2021; Avak et al., 2019) disturbing the original signal. Prolonged events can even fully compromise the preservation of the climatic information contained by ice cores. Avak et. al., (2019) showed that atmospheric composition was well preserved in an Alpine ice core during the winter, but that the melting in the spring and early summer caused a preferential loss of certain major ions and trace elements. In particular, the elution behavior of major ions is most likely controlled by redistribution processes occurring during snow metamorphism, as underlined by recent work investigating the distribution of impurities within the ice matrix (Bohleber et al., 2021). Variable mobility has also been observed for trace elements, although they have been suggested to be better preserved than major ions (Avak et al., 2019). Since the temperature is below the melting point (<0°C) throughout the year, the Antarctic and the Greenland plateau are the best locations for such studies, nevertheless, rare melting events have been observed in the Greenland plateau (Bonne et al., 2015). ~~However, ice cores retrieved from these locations do not provide more regional climatic information. To overcome this limitation,~~ Beyond the polar regions, many other drilling sites have been investigated, including the Alps (Arienzo et al., 2021; Gabrielli et al., 2016; Schwikowski et al.,

1999), the Himalayas (Thompson et al., 2018; Dahe et al., 2000), the Andes mountain range (Hoffmann et al., 2003; Thompson et al., 2021), the Canadian Arctic (Zdanowicz et al., 2018) and the Svalbard archipelago (Isaksson et al., 2005; Wendl et al., 2015).

There are several ice caps in Svalbard, but given their relatively low altitude, most are not suitable for the preservation of a pristine climate archive. The glacier equilibrium line altitude (ELA) varies across the different regions of the archipelago but is generally situated between 300 to 700 m a.s.l.(van Pelt et al., 2019). In the southern part of the archipelago, the ELA is lower due to the higher winter snow accumulation, while in the northern part, the ELA rises to 600-700 m. Signal preservation requires drilling to be above the ELA, for regular snow accumulation, but also, so that summer percolation only moderately affects the upper firn layers.

Several drilling operations have collected ice core records in the archipelago, in particular in the northern part. The longest (in time coverage) ice-core record was collected from Lomonosovfonna, at 1230 m a.s.l., and covered ~1200 years of Svalbard climate history (Divine et al., 2011). Other ice cores have been retrieved from Austfonna (750 m. a.s.l.), covering approximately 900 years (Watanabe et al., 2001), Vestfonna (600 m a.s.l.) covering approximately 500 years (Matoba et al., 2002) and Holtedahlfonna (1140 m a.s.l.) covering approximately 300 years (Beaudon et al., 2013).

To assess the reliability of Svalbard ice cores for future climate studies, we conducted an analysis of the oxygen isotopic composition ($\delta^{18}O$) from a series of four shallow ice cores collected at the summit of the Holtedahlfonna ice field. These ice cores were obtained in different years and cover overlapping atmospheric deposition periods, offering insights into the evolution of isotopic stratigraphy over time. Our primary focus in this study was on $\delta^{18}O$ because it is a widely utilized parameter in ice core science for reconstructing past temperature changes (Divine et al., 2011; Stenni et al., 2017). Furthermore, it is comparatively less influenced by melting and percolation events (Pohjola et al., 2002), as compared to other chemical parameters analyzed in ice cores. Numerous prior investigations have been conducted using shallow ice cores from the Holtedahlfonna summit, exploring various elements and compounds. These studies have consistently highlighted the site's significance for climate research (Burgay et al., 2021; Barbaro et al., 2017; Spolaor et al., 2013a; Ruppel et al., 2017). Our study results were correlated with glacier mass balance measurements and snowpack modeling. Notably, we observed a gradual degradation of the climate signal, although the long-term (>5 years) climate variations still appear to be preserved. This underscores the urgency of obtaining records that can enhance our understanding of the climate processes occurring in one of the most rapidly changing environments on our planet.

## 2. Methodology

## 2.1 The Holtedahlfonna ice field

Holtedahlfonna (HDF – Figure 1) is the largest ice field (ca. 300 $km^2$) in northwestern Spitsbergen, located about 40 km from the Ny-Ålesund research station. It covers an elevation range of 0–1241 m a.s.l. (Nuth et al., 2017) and the upper part of the glacier, located approximately at 1100 m a.s.l., has a positive annual snow mass balance, ca. +0.50 m. w.e. $a^{-1}$(Beaudon et al., 2013; van Pelt et al., 2019). The site has already been studied for long term paleoclimate reconstruction, covering the past 300 years (Divine et al., 2011; Goto-Azuma et al., 1995). In April 2005, a 125 m a long ice core was drilled using an electromechanical corer and the bottom temperature in the borehole was –3.3°C, assuring cold ice conditions over the entire ice thickness. Ice temperature measured in the borehole featured a maximum of –0.4°C at 15 m depth, indicative of firn-warming due to the release of latent heat from refreezing (Beaudon et al., 2013).

## 2.2 The Holtedahlfonna shallow firn cores: collection and processing

In the spring seasons of 2012, 2015, 2017 and 2019, a total of four shallow cores were obtained from the summit of the Holtedahlfonna ice field (79°09′N, 13°23′E; 1150 m. a.s.l.). The shallow cores were collected using a 4″ fiberglass Kovacs Mark-II ice corer driller powered by an electric drill and reached depths of 7-10 m into the firn. All shallow cores were drilled from the bottom of the annual snowpack\last summer surface. Length and density of each firn core section were logged, stored in plastic sleeves, and transported back to Ny-Ålesund for laboratory analysis. For cores collected in 2012, 2017 and 2019, core samples were processed in a class-100 laminar flow hood in the laboratory of the Italian research station "*Dirigibile Italia*" in Ny-Ålesund. Core sections were cut into pieces of 5 to 7 cm length using a ceramic knife and the external part of the core physically removed to avoid contamination. The density was measured for each sample produced. The core 2015 was processed as reported in Ruppel et al. (2017).

## 2.3 Oxygen stable isotope analysis ($\delta^{18}O$)

The samples for oxygen isotopic analyses ($\delta^{18}O$) were melted at room temperature (≈20°C) and transferred into 2-mL clear glass vials filled to the top. Samples were kept refrigerated at +4°C and analyzed at Ca Foscari University of Venice (2017 and 2019) and at Tallinn University of Technology (2012 and 2015). In both cases, the isotopic measurements were carried out using a Picarro L1102-*i* analyser coupled with a CTC Pal autosampler. The instrument uses Cavity Ring-Down Spectroscopy (CRDS) technology, based on the unique near-infrared absorption spectrum of each gas-phase molecule. The autosampler injects the melted sample into the vaporizer (set at 110°C), where it becomes gaseous and is then transferred into the cavity (nitrogen is used as a carrier), in which the measurement occurs. The instrument datasheet reports an analytical precision of ± 0.10 δ‰ for $\delta^{18}O$.

Each sample was injected eight times: only results within ± σ from the 8-repetition average were kept for records, while outliers were discarded. Internal isotopic standards periodically calibrated against IAEA-certified standards (V SMOW 2 and SLAP 2) were used for calibration.

### 2.4 Holtedahlfonna surface mass balance

Surface mass balance (SMB) of Holtedahlfonna is monitored by the Norwegian Polar Institute (Kohler, 2013). SMB is obtained from repeated field visits at the end of winters and summers, with winter snow-depth sounding and density measurements and repeated height readings of an array of stakes along the glacier centerline. Balance estimates are extrapolated over the entire glacier basin by determining the balance as function of elevation and averaging them, applying weights determined from the distribution of glacier area as a function of elevation. This method quantifies the glacier-wide SMB, i.e., the mass changes at the surface of the glacier, and within near-surface layers, but does not include internal mass changes below the last summer surface. SMB measurements at Holtedahlfonna started in 2003; since the drilling site is in the accumulation area, these measurements provide information of the seasonal accumulation, but disregard the internal accumulation that may occur due to refreezing of meltwater in layers below the last summer surface. The uppermost part of HDF has had a consistently positive mass balance and is therefore assumed to preserves most of its annual snow deposition.

### 2.5 Estimation of Meteorological condition at the summit of the Holtedahlfonna ice field

In absence of in-situ meteorological measurements at the drill site, we obtained long-term seasonal (DJF, MAM, JJA and SON) temperature and precipitation series from the high-resolution CARRA dataset (Copernicus Arctic Regional Re-Analysis, Schyberg et al., 2020). This 2.5 km resolution product covering the period 1991-2020 is downscaled from ERA5(Hersbach et al., 2020) using the state-of-the-art weather prediction model HARMONIE-AROME (Bengtsson et al., 2017). CARRA has several improvements compared to ERA5, including assimilation of a large amount of additional surface observations, extensive use of satellite data, and improved representation of sea ice; it is therefore likely to provide the best estimate of meteorological conditions in the Barents Sea region. The CARRA reanalysis is also used to force the CryoGrid community model (Westermann et al., 2023) to simulate glacier mass balance, seasonal snowpack evolution and meltwater runoff across Svalbard Franz-Joseph Land and Novaya Zemlya. The model couples the surface energy balance and a multi-layer subsurface module to resolve meltwater production, percolation, storage, refreezing and runoff, accounting for the interaction with local density and temperature stratigraphers. The vertical

discretization comprises 47 layers of variable vertical extend to cover the uppermost 20 m below the surface (Steffensen Schmidt et al., 2023).

## 3.RESULTS

### 3.1 Shallow firn core dating and alignment

To date the core, we use the seasonal cycle (where present) of the $\delta^{18}O$ data together with the mass balance data available since 2003. Core depths were converted to water equivalent using the density data acquired during the core processing. Density for the 2015 core is taken from Ruppel et al., (2017), the 2012 values are published in Spolaor et al., (2013b), and density for the 2017 and 2019 cores are presented in this work; density profiles of the four shallow cores (Figure S1) all reveal a similar pattern.

The cores were collected within 50 m of the mass balance stake HDF-10. The stake measurements, which show a consistently net positive mass balance, provide a historical record of snowpack accumulation that can be directly used to assign a specific year to firn core depth range (Figure 2). Oxygen stable isotopes can be used independently to annually date the ice, but only in ice-core archives where the seasonal signal is well preserved. This means that snow accumulation needs to be sufficiently high, and the summer ablation should not compromise the stratigraphy by redistributing and smoothing the original atmospheric signal. By combining the annual accumulation and the core depth expressed in water equivalent and the seasonality of $\delta^{18}O$ (where available and preserved), we can date and align all four cores (Figure 3).

The cores cover 14 years in total (from 2005 to 2018). The time coverage for each core is reported in Table 1 together with additional information for each firn core. The 2012 core had a $\delta^{18}O$ average value of -15.3 ± 1.0 ‰, the 2015 core a value of -15.1 ± 0.8 ‰, the 2017 core an average value of -14.4 ± 0.7 ‰ and the 2019 core an average value -14.1 ± 1.2 ‰. Specific features overlap in the four cores (Figure 3 and 6), and show a general increasing trend in $\delta^{18}O$ from 2005 until 2018. In particular, the 2012 and 2015 cores have similar fluctuations with shared features, particularly during 2005-2006, which was used for core alignment. They also showed similar features in the remaining periods that they each covered, though with minor differences. The high $\delta^{18}O$ values in 2013 that occurred in the 2015 core are also clearly found in the 2017 core, helping to synchronize the records. The alignment of the 2019 core with previous cores could only be done through mass balance values, since the $\delta^{18}O$ values did not show the same peaks as the other records. In particular, the decrease in $\delta^{18}O$ values recorded in the period representing 2016 was not present in the 2017 core.

### 3.2 Meteorological condition at the Holtedahlfonna ice field summit

The meteorological conditions at the Holtedahlfonna ice field summit from 1991 to 2020 were retrieved from model re-analysis and provide a clear overview of the on-going changes occurring at the site.

The annual average winter temperatures (DJF) at the HDF summit (located at 1100 m a.s.l.) ranged from -25°C to -15°C, and show an increasing trend of 2.37°C per decade for the period 1991–2020 (Figure 4a - blue line). The annual average spring and summer temperatures (MAM) ranged from -17°C to -12°C (Figure 4a - green line) and -5°C to -1°C (Figure 4a - red line), respectively. The average temperature increase per decade since 1991 was 0.38°C for spring and 0.51°C for summer. The temperature during fall (SON) increased by 1.47 °C per decade and ranged from -15°C and -5°C (Figure 4a - brown line).

Although the average seasonal summer temperatures were below the water melting point, positive degree days (PDD – Figure 4b, expressed as the sum of mean daily temperatures for all days during a period where the temperature is above 0°C), occurred at the summit of HDF, causing snowpack melting. The cumulative annual PDD, retrieved from model temperature series outputs, showed a stable value for the period 1990 to 2015, although some years (1994, 1999, 2010) and periods (2001–2006) were characterized by an increased PDD. A net increase from 2015 to the present time was recorded. Snow melting at the site was clearly visible and confirmed by the presence of several ice lenses in the core (Spolaor et al., 2013b; Burgay et al., 2021).

The annual model estimated precipitation (1991–2020) ranged between 630 to 1170 mm w.e. per year, with a slight increase in the most recent period (Figure 4d). A similar trend was also observed in Ny-Ålesund (Førland et al., 2020). Seasonal precipitation (Figure S2) was most abundant during fall (SON) and winter (DJF), with an average precipitation of 286 mm w.e. and 274 mm w.e, respectively, and a relative average contribution of 32% and 31%, respectively, to the total deposition. The lowest precipitation occurred in spring (MAM) and summer, with an average precipitation of 170 mm w.e. and 145 mm w.e., respectively, which represents an average contribution of 20% of the total deposition in spring and 17% of the total precipitation in summer.

Although the annual mass balance was always positive, the summer mass balance was both positive and negative depending on the meteorological conditions (Figure 2). The winter accumulation represented between 60% and 100% of the net annual mass balance at the site. Even though the summer mass balance data from 2015 to 2020 were positive, melting also occurred and water percolated into the snow and firn before refreezing.

Most of the melting occurred during the summer period (JJA), but melting events also occurred during fall and late spring (Figure S3). The estimated annual melting at the site from 1991-2020 (Figure 4c) varied between 960 mm w.e (2020) and 117 mm w.e (2008) and showed a clear increasing tendency

following temperature rise. Moreover, autumn snowpack melting events, previously rare, became a more regular phenomenon in the period 2015 to 2019. However, spring snowmelt is sporadic (2011) and rare.

In addition to meteorological reanalysis from the HARMONIE-AROME model, the CryoGrid simulation provided information about the presence of liquid water in the firn and its penetration (Figure 5). Percolation was mainly confined to the surface layer between 1991 (beginning of the simulation) to the end of the 90s(except 1999). Percolation increased significantly from 2000 onwards. In particular, for the period 2004-2005, severe surface melt events occurred (Figure 2c and Figure S3), causing water percolation for several meters (Figure 5). The 2006 to 2014 period was characterized by relatively limited surface melting and the lowest amount of percolated water, which did not exceed one (2006 and 2008) to four (2010 and 2011) annual snow accumulation periods. Based on the model's calculations, water percolation increased since 2014 and was able to reach deeper firn strata. Although the model suggests the presence of liquid water in the firn, water and elution channels are complex to simulate and likely present high spatial variability. Hence, we only consider the data presented in Figure 5 in a qualitative manner to evaluate the possible presence or absence of liquid water within the snowpack and its theoretical penetration\percolation depth.

## 4. DISCUSSION

The aim of this paper is to evaluate the effect of temperature rise on the $\delta^{18}O$ Holtedahlfonna ice core signal preservation. Our discussion will focus only on the periods covered by the shallow cores.

Based on the $\delta^{18}O$ records of the four shallow cores, it is evident that the seasonal signal experienced considerable changes and progressively deteriorated in the most recent cores. While wind redistribution can move snow, it primarily affects snow deposited at similar altitudes, which tends to have a similar water stable isotope fingerprint. It is highly improbable that snow deposited at lower elevations could be lifted and deposited at the summit of Holthedalfonna in quantities significant enough to completely degrade the climate signal preserved in the ice. Moreover, analysis of wind patterns in Ny-Ålesund does not indicate any significant shifts or changes in average wind velocities (Cisek et al., 2017).

In our discussion we suggest that the most important parameters affecting the pristine atmospheric signal trapped in the snow is the amount of snow melting, which depends on the snow and meteorological conditions, and the penetration of the melt water into the snowpack.

In the core collected in 2012 (Figure 3), the seasonal variations are clear for almost the entire period except for 2004-2005, a period characterized by significant summer melt that disturbed the

atmospheric signal trapped in the ice. However, for the period 2006-2011, the seasonality is clear and each $\delta^{18}O$ seasonal cycle is confined within the annual snow mass balance measurements.

The 2015 core still presented the seasonal cycle in the upper half of the core, corresponding to the second period (2010-2014). However, the seasonal feature of the $\delta^{18}O$ identified in the 2012 core for the periods 2008–2009 was no longer present, suggesting a possible elution caused by the percolation of liquid water (Figure 5). The model simulation supports the possibility that post deposition events may have occurred within the firn due to the percolation of liquid water.

The most striking change in terms of the $\delta^{18}O$ seasonal cycle occurred in the 2017 core. The 2017 core overlapped with the 2015 core for the period 2012-2014 and, while the seasonality for this period was well defined in the 2015 core, only the seasonal $\delta^{18}O$ for year 2013 was visible in the 2017 core. The $\delta^{18}O$ seasonal cycle of 2014 has undergone significant smoothing and the $\delta^{18}O$ seasonal cycle in 2012 is no longer visible. For the period 2015-2016, the seasonal cycle was not clear, although oscillations were still present.

In the most recent core collected in 2019, a seasonal $\delta^{18}O$ cycle could no longer be detected and particular features, such as the drop in the $\delta^{18}O$ signal in 2016 (not observed in the 2017 core), was not linked to a drop in the temperature, since 2016 was the warmest year on record (Figure 6, red dots).

Two independent statistical analyses, one using the significant value of a regression model and the other using the spectral analysis, were performed on the shallow core records to test the presence of seasonal oscillation on the $\delta^{18}O$ signal. Both statistical analyses demonstrated the disappearance of the seasonal signal in the most recent (2017 and 2019) shallow cores (full details are reported in the supplementary material - section 2). Using the Linear regression model for each core and each year, we first identified the maximum and the minimum for the $\delta^{18}O$ signal (Figure 6) and then calculated the weighted slope between each extreme value (Figure 7). The significant values of the seasonality of the weighted slope considering the increasing and decreasing periods separately is presented in Table S1. A significant seasonality (p-value < 0.05) is only observed in 2012 and 2015 ice cores.

The change in seasonality and, to a lesser extent, in the total amount of precipitation, might have influenced the $\delta^{18}O$ signal of the four cores. However, from the model results, the seasonal contribution to the total annual precipitation did not change significantly (Figure S2). This would suggest that precipitation does not play a central role in explaining the degradation, or possible change, in the $\delta^{18}O$ signal, and that increased melting and water percolation might have had a larger effect. Instead, the increase in year-round precipitation could enhance melt water formation during the summer periods. The preservation of the ice core climate signal strongly depends on the amount of snow melt during summer and the capability of water to penetrate the snowpack, which in turn is

controlled by snow temperature. The progressive atmospheric warming, the increase of summer melting and water percolation as well as the water movement within the snowpack could all have had an impact on the $\delta^{18}O$ signal present in the Holtedahlfonna firn\ice.

The progressive degradation and loss of the seasonality of the $\delta^{18}O$ signal in the shallow core (2004 - 2018) is also supported by the results obtained from the $\delta^{18}O$ signal in the 2005 core. In the deep core collected in 2005, the seasonal signal of the $\delta^{18}O$ in the period 1960 to 2000 was well preserved (Figure S5). The signal determined in the 2005 Holtedahlfonna deep ice core shared similar features with those determined in the 2012 and 2015 shallow cores, where the seasonal oscillations were still partially present, but not with signals determined in the 2017 and 2019 cores, where the seasonality in $\delta^{18}O$ almost disappeared. We suggest that since 2015, estimated melting and percolation increased because of the evolution of the general atmospheric conditions, causing a deterioration of the climate signal preserved in the firn\ice.

Water stable isotopes are commonly used as a temperature proxy. By overlapping the water stable isotope profiles measured in the shallow cores and, comparing their trends with the annual average temperature, we suggest that the general atmospheric temperature trend is still preserved within the HDF ice (Figure 8), although some clear deterioration is visible. For example, the highest annual temperature values recorded in 2016 were not mirrored in the $\delta^{18}O$ record from the 2017 and 2019 cores. This underscores the impact of high temperatures on the preservation of pristine atmospheric signals in ice cores that have significantly impacted the preservation of the atmospheric signal, since temperature values.

## 5. Conclusion

An ice core drilled at the summit of Holtedahlfonna has previously been used to provide atmospheric and climate conditions about the past 300 years (Beaudon et al., 2013). Before 2005, the site was characterized by moderate summer melting, yet the snow and ice analysed proved to preserve important climate information as well as the main seasonal features. The current warming of the Svalbard archipelago has clearly enhanced glacial mass loss, with a rise in the equilibrium line altitude and a shorter snow season. This study is the first investigating the impact of temperature rise on climate signal preservation within the firn\ice in one of the highest ice fields in Svalbard. The direct effect of higher temperatures has increased summer melt and enhanced meltwater percolation. In this study, we have shown that the climate signal preserved in the ice has been progressively deteriorated. For example, in seven years, the seasonal signal visible in the 2012 core has completely disappeared in the 2019 core, most likely due to increased snow summer melting and water percolation. However, although the $\delta^{18}O$ seasonal signal has disappeared, the overall atmospheric

warming signature is still preserved in the ice\firn, suggesting that the site is still suitable for long record paleoclimate reconstruction. However, with the current warming rate of the Svalbard archipelago and the consequent increase in summer melting, Holtedahlfonna and other ice fields at similar altitudes might no longer provide suitable records of the climatic condition. Glaciers worldwide are currently not only losing mass at unprecedented rates, but also the climatic information they contain.

**Acknowledgments**

This work has been supported by the "Programma di Ricerca in Artico" (PRA, project number PRA2019-0011, Sentinel); by the Svalbard Science Forum/Research Council of Norway through the Arctic Field Grant call (project ASIHAD, ISSICOS, BIOMASS), by French Polar Institute IPEV (Institut Polaire Français Paul-Emile Victor) science funding (programs 399 and 1192) and the Svalbard Strategic Grant (project C2S3, nr. 257636, SnowNet nr. 295779 and BC3D nr. 283466). This project has received funding from the European Union's Horizon 2020 research and innovation programme under grant agreement no. 689443 via project iCUPE (Integrative and Comprehensive Understanding on Polar Environments). This research has been partially funded by the University of Perugia Research Action no. 5 "Climate, Energy, and Mobility". Cryogrid simulations have been supported by the Nansen Legacy project (Research Council of Norway grant 276730) and SIOS infraNor (Research Council of Norway grant 269927).

**Author contribution**

AS, EB, FS, JCG, CL, MB, JG, FB, and DC conceived the experiment and collected the samples and wrote the paper with the support of all co-authors; CT, TM, GD and BS analyze the samples; JK provide the field mass balance data and contribute in data interpretation; LSS and TVS provide the model data and atmospheric re-analysis; FdB and MC perform the statistical exercise and contribute in data interpretation. BL and FD contribute to data interpretation. DD and EI provide the data from previous ice core and contribute to data interpretation.

**Data availability**

The data will be available upon request to the corresponding author.

**Competing interests**

The authors declare that they have no conflict of interest.

## FIGURES

**Figure 1.** Location of the drilling site (red star) within the Holtedahlfonna (HDF) ice field as compared to the Ny-Ålesund research village (NyA). Maps from https://toposvalbard.npolar.no (last access: 5th June 2023).

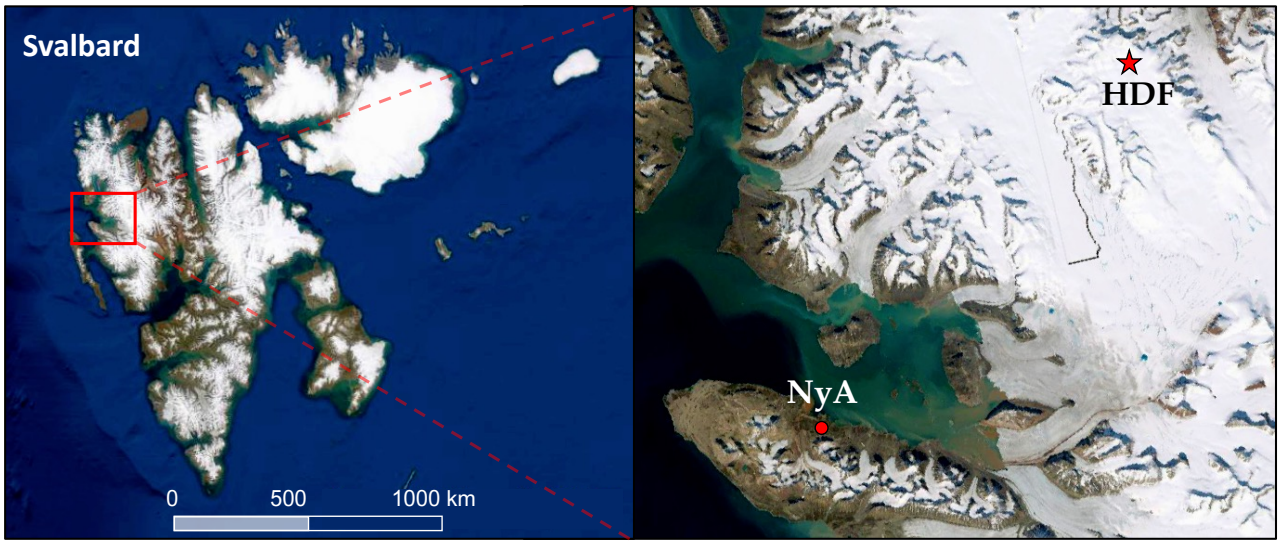

**Figure 2.** Mass balance measurements, modelled precipitation and snow melt at the drilling site. a) cumulative surface mass balance (SMB) expressed in cm of w.e., b) comparison of modeled total annual precipitation (green – in mm w.e) and modeled melt (red in mm w.e). c-e) net, winter and summer mass balance (cm w.e.) measured at the top of the Holtedahlfonna ice field, respectively.

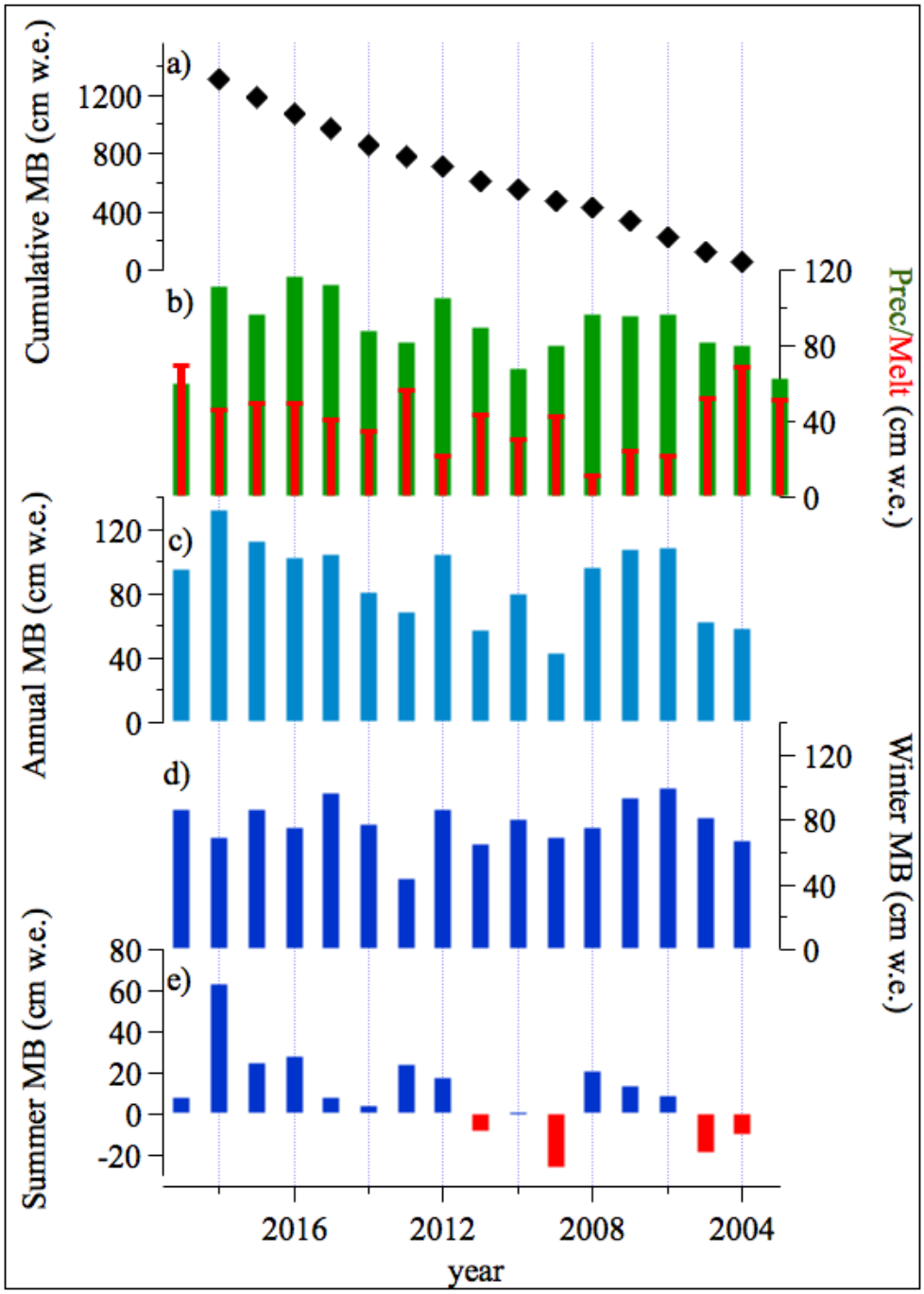

**Figure 3. Oxygen stable isotope profiles** $\delta^{18}O$ of the shallow cores. The shallow core was aligned by converting the depth to depth expressed in cm of w.e. using the annual mass balance (MB) data. The white and pink colors distinguish different years based on the MB measurements and are reported in the upper panel. The "0 cm" value refers to the last summer snow surface.

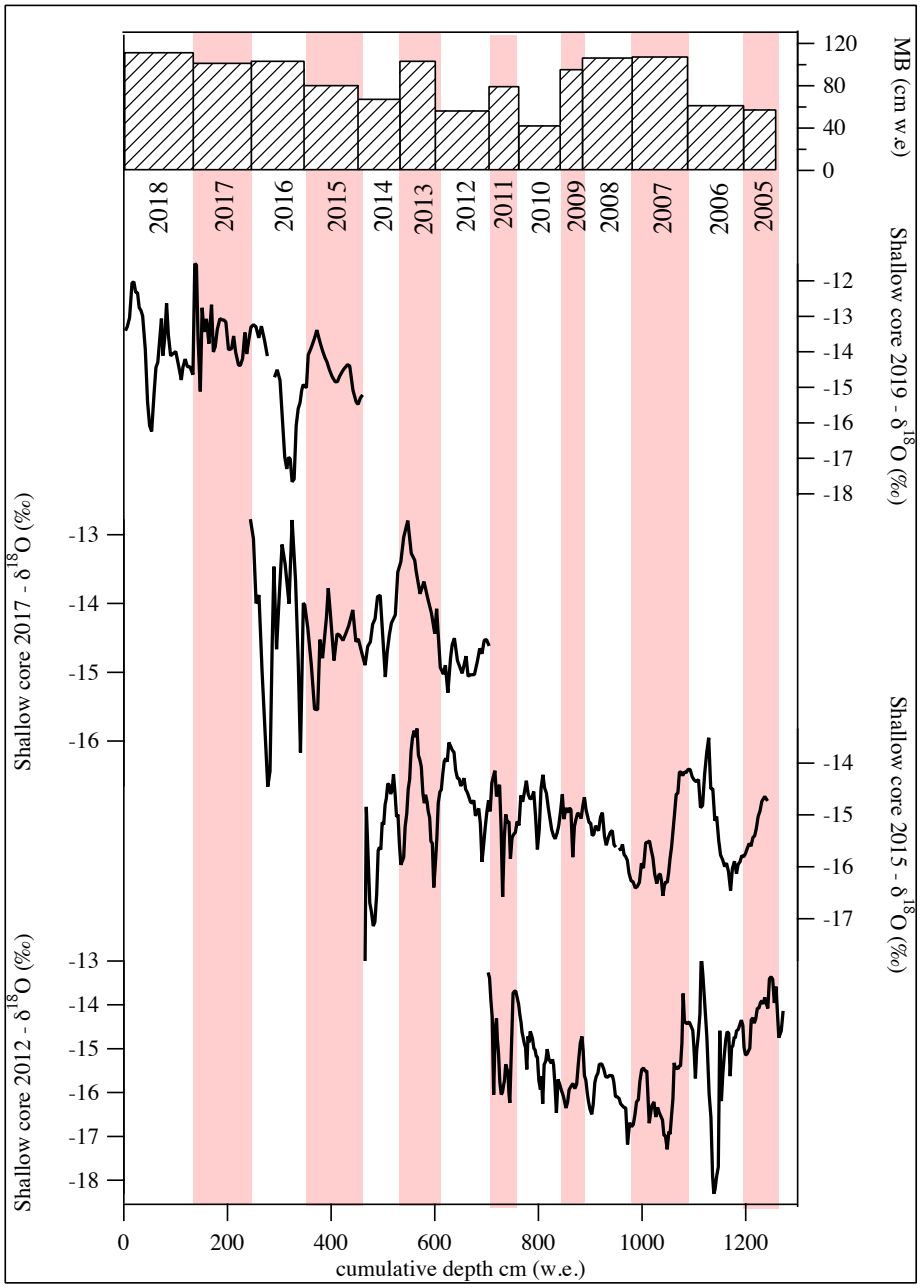

**Figure 4.** Modeled meteorological conditions at the Holtedahlfonna shallow core drilling site (1150 m a.s.l.) from 1991 to 2020 at seasonal resolution. a) winter (DJF - blue), spring (MAM – green), summer (JJA – red) and fall (SON – brown) temperatures, with increasing trend line for the period investigated. b) annual PDD value (grey). c) annual melting (in mm w.e in red). d) annual total precipitation (in mm w.e. – blue)

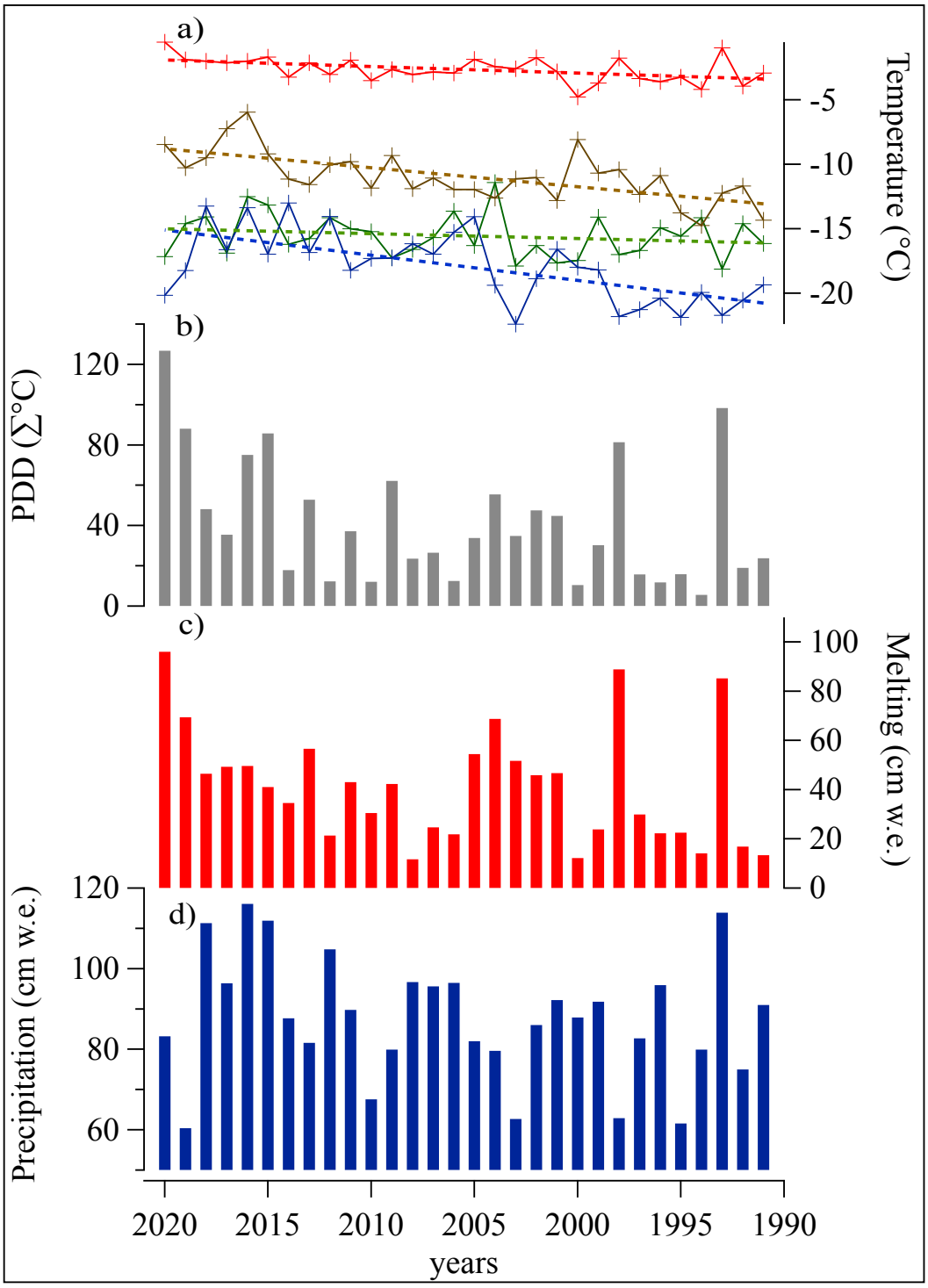

**Figure 5.** Evolution of the water content in the snowpack at the top of Holtedahlfonna estimated by model simulation between 1990 and 2020. The chart shows the volumetric water content (%) in the snow/firn (white to blue color), surface height evolution (black line), 0° C isotherm (red). Dashed lines show the period covered by the four shallow cores.

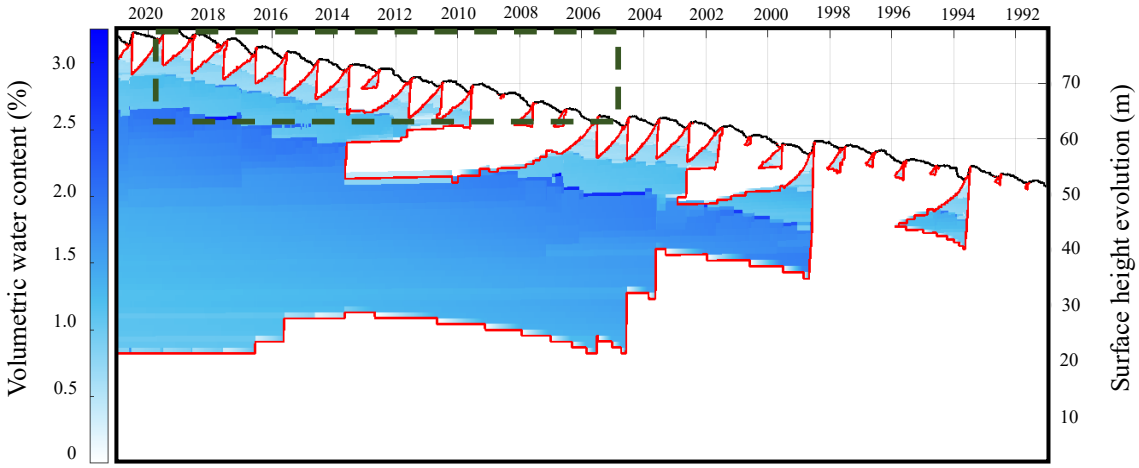

559 **Figure 6**. Identification of the annual minimum and maximum values of $\delta^{18}O$ (red and blue points)
560 based on the annual mass balance dating for the four shallow cores (panel a – 2012 core, panel b –
561 2015 core, panel c – 2017 core, panel d – 2019 core).

562

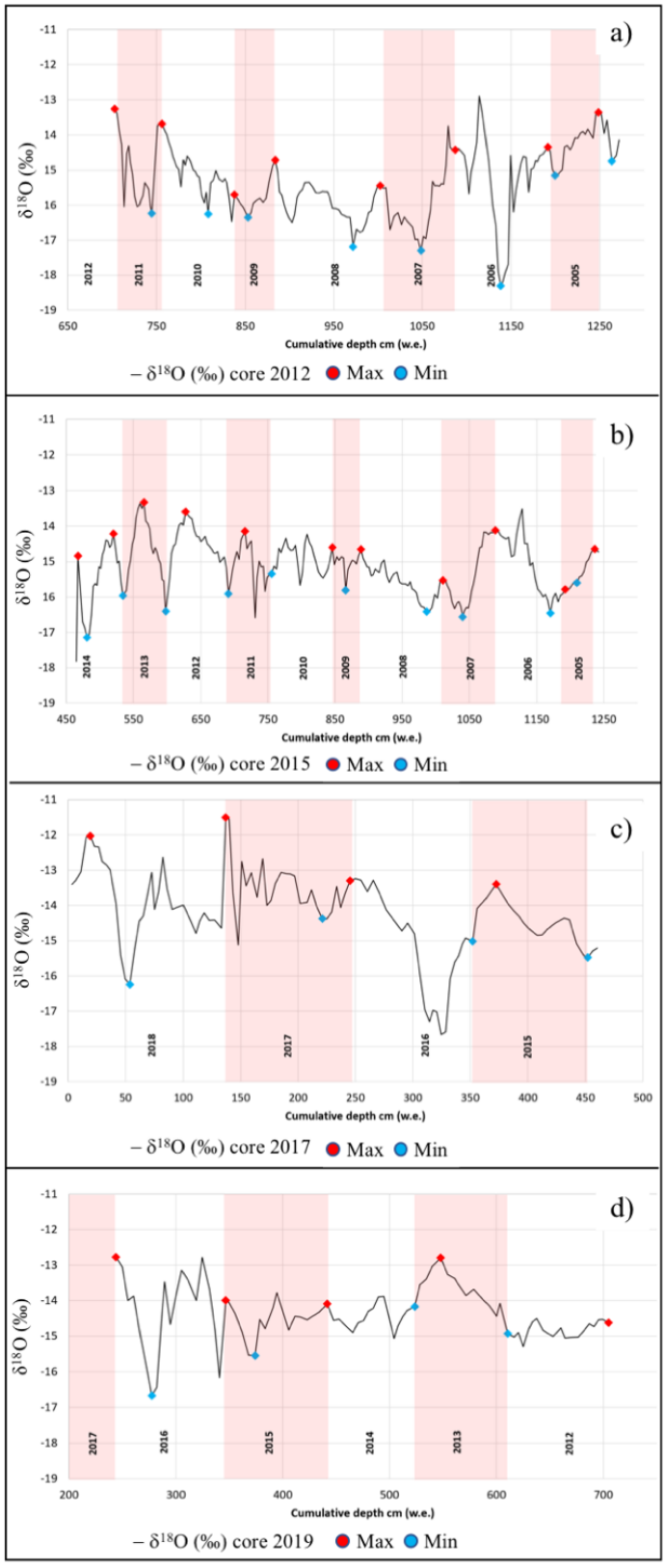


563
564

**Figure 7.** Representation of the slope between the annual maximum and minimum value of $\delta^{18}O$ weighted on the percent difference in the value of $\delta^{18}O$ for each annual mass balance for the four shallow cores. The black line represents the trend of weighted slope change along the years (panel a – 2012 core, panel b – 2015 core, panel c – 2017 core, panel d – 2019 core).

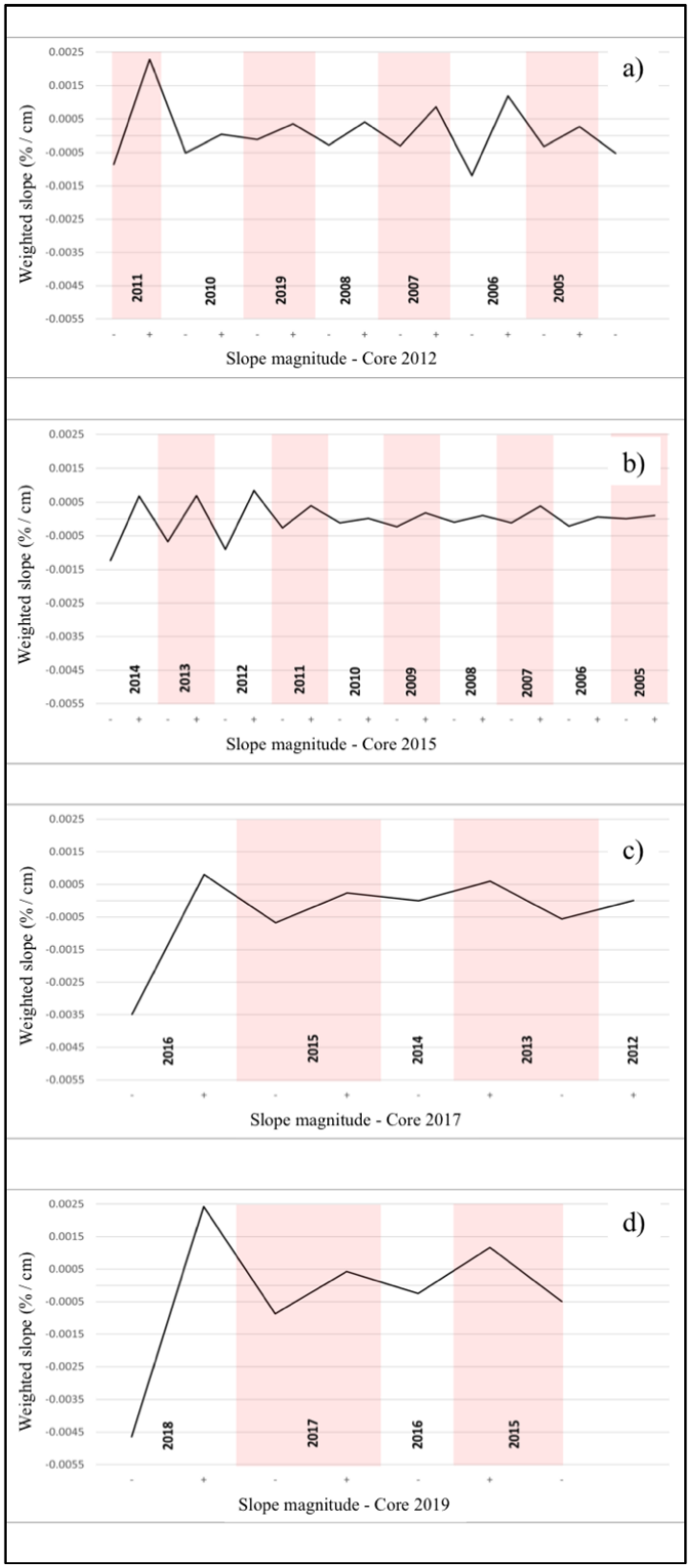

**Figure 8.** Estimated annual average temperature at the top of Holtedahlfonna ice field (black square) obtained from the monthly atmospheric re-analysis data as describe in section 2.5 and presented in figure S4. The circles representing the $\delta^{18}O$ signal of the four shallow cores (black circle for the 2012 core, green circles for the 2015 core, blue circle for the 2017 core and red circle for the 2019 core).

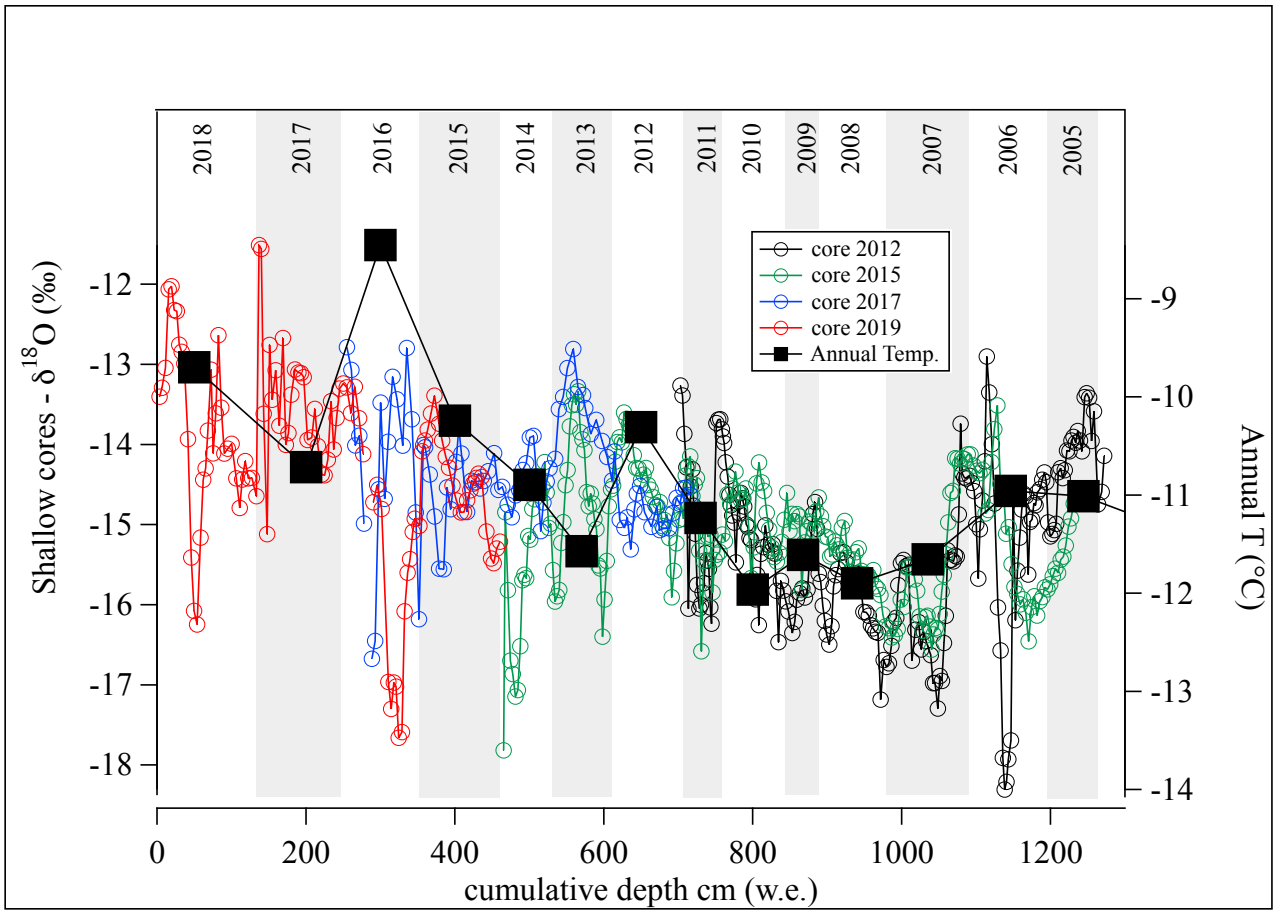

## TABLES

**Table 1**. Shallow ice core descriptions. The table reports the length expressed in cm and in water equivalent (w.e.) and the estimated (Est. start year\Est. end year) time coverage. The average density of the cores is also reported.

| Core ID | Length (cm) | Length (cm w.e.) | Ave density ($kgL^{-1}$) | Est. Start year | Est. End year | Drilling period | Reference |
|---|---|---|---|---|---|---|---|
| 2019 | 769 | 461 | 0.60 | 2018 | 2012 | April 2019 | This work |
| 2017 | 736 | 466 | 0.63 | 2016 | 2010 | April 2017 | *Burgay et a. 2017* |
| 2015 | 1185 | 832 | 0.70 | 2014 | 2005 | May 2015 | *Ruppel et al. 2017* |
| 2012 | 954 | 575 | 0.60 | 2011 | 2005 | April 2012 | *Spolaor et al. 2013* |

## REFERENCES


Arienzo, M. M., Legrand, M., Preunkert, S., Stohl, A., Chellman, N., Eckhardt, S., Gleason, K. E., and McConnell, J. R.: Alpine Ice-Core Evidence of a Large Increase in Vanadium and Molybdenum Pollution in Western Europe During the 20th Century, Journal of Geophysical Research: Atmospheres, 126, https://doi.org/10.1029/2020JD033211, 2021.

Avak, S. E., Trachsel, J. C., Edebeli, J., Brütsch, S., Bartels-Rausch, T., Schneebeli, M., Schwikowski, M., and Eichler, A.: Melt-Induced Fractionation of Major Ions and Trace Elements in an Alpine Snowpack, J Geophys Res Earth Surf, 124, 1647–1657, https://doi.org/10.1029/2019JF005026, 2019.

Barbaro, E., Spolaor, A., Karroca, O., Park, K.-T., Martma, T., Isaksson, E., Kohler, J., Gallet, J. C., Bjorkman, M. P., Cappelletti, D., Spreen, G., Zangrando, R., Barbante, C., and Gambaro, A.: Free amino acids in the Arctic snow and ice core samples: Potential markers for paleoclimatic studies, Science of the Total Environment, 607–608, https://doi.org/10.1016/j.scitotenv.2017.07.041, 2017.

Beaudon, E., Moore, J. C., Martma, T., Pohjola, V. A., van de Wal, R. S. W., Kohler, J., and Isaksson, E.: Lomonosovfonna and Holtedahlfonna ice cores reveal east–west disparities of the Spitsbergen environment since <scp>AD</scp> 1700, Journal of Glaciology, 59, 1069–1083, https://doi.org/10.3189/2013JoG12J203, 2013.

Beaudon, E., Moore, J. C., Martma, T., Pohjola, V. A., van de Wal, R. S. W., Kohler, J., and Isaksson, E.: Lomonosovfonna and Holtedahlfonna ice cores reveal east–west disparities of the Spitsbergen environment since AD 1700, Journal of Glaciology, 59, 1069–1083, https://doi.org/10.3189/2013JoG12J203, 2017.

Bengtsson, L., Andrae, U., Aspelien, T., Batrak, Y., Calvo, J., de Rooy, W., Gleeson, E., Hansen-Sass, B., Homleid, M., Hortal, M., Ivarsson, K.-I., Lenderink, G., Niemelä, S., Nielsen, K. P., Onvlee, J., Rontu, L., Samuelsson, P., Muñoz, D. S., Subias, A., Tijm, S., Toll, V., Yang, X., and Køltzow, M. Ø.: The HARMONIE–AROME Model Configuration in the ALADIN–HIRLAM NWP System, Mon Weather Rev, 145, 1919–1935, https://doi.org/10.1175/MWR-D-16-0417.1, 2017.

Boers, N.: Early-warning signals for Dansgaard-Oeschger events in a high-resolution ice core record, Nat Commun, 9, 2556, https://doi.org/10.1038/s41467-018-04881-7, 2018.

Bohleber, P., Roman, M., Šala, M., Delmonte, B., Stenni, B., and Barbante, C.: Two-dimensional impurity imaging in deep Antarctic ice cores: snapshots of three climatic periods and implications for high-resolution signal interpretation, Cryosphere, 15, 3523–3538, https://doi.org/10.5194/tc-15-3523-2021, 2021.

Bonne, J.-L., Steen-Larsen, H. C., Risi, C., Werner, M., Sodemann, H., Lacour, J.-L., Fettweis, X., Cesana, G., Delmotte, M., Cattani, O., Vallelonga, P., Kjær, H. A., Clerbaux, C., Sveinbjörnsdóttir, Á. E., and Masson-Delmotte, V.: The summer 2012 Greenland heat wave: In situ and remote sensing observations of water vapor isotopic composition during an atmospheric river event, Journal of Geophysical Research: Atmospheres, 120, 2970–2989, https://doi.org/10.1002/2014JD022602, 2015.

Burgay, F., Barbaro, E., Cappelletti, D., Turetta, C., Gallet, J.-C., Isaksson, E., Stenni, B., Dreossi, G., Scoto, F., Barbante, C., and Spolaor, A.: First discrete iron(II) records from Dome C (Antarctica) and the Holtedahlfonna glacier (Svalbard), Chemosphere, 267, 129335, https://doi.org/https://doi.org/10.1016/j.chemosphere.2020.129335, 2021.

Cisek, M., Makuch, P., and Petelski, T.: Comparison of meteorological conditions in Svalbard fjords: Hornsund and Kongsfjorden, Oceanologia, 59, 413–421, https://doi.org/10.1016/j.oceano.2017.06.004, 2017.

Dahe, Q., Mayewski, P. A., Wake, C. P., Shichang, K., Jiawen, R., Shugui, H., Tandong, Y., Qinzhao, Y., Zhefan, J., and Desheng, M.: Evidence for recent climate change from ice cores in the central Himalaya, Ann Glaciol, 31, 153–158, https://doi.org/10.3189/172756400781819789, 2000.

694 Dahlke, S. and Maturilli, M.: Contribution of atmospheric advection to the amplified winter warming
695 in the arctic north atlantic region, Advances in meteorology,
696 https://doi.org/10.1155/2017/4928620, 2017.
697 Dahlke, S., Hughes, N. E., Wagner, P. M., Gerland, S., Wawrzyniak, T., Ivanov, B., and Maturilli,
698 M.: The observed recent surface air temperature development across Svalbard and concurring
699 footprints in local sea ice cover, International Journal of Climatology, 40, 5246–5265,
700 https://doi.org/https://doi.org/10.1002/joc.6517, 2020a.
701 Dahlke, S., Hughes, N. E., Wagner, P. M., Gerland, S., Wawrzyniak, T., Ivanov, B., and Maturilli,
702 M.: The observed recent surface air temperature development across Svalbard and concurring
703 footprints in local sea ice cover, International Journal of Climatology, n/a,
704 https://doi.org/10.1002/joc.6517, 2020b.
705 Divine, D., Isaksson, E., Martma, T., Meijer, H. A. J., Moore, J., Pohjola, V., van de Wal, R. S. W.,
706 and Godtliebsen, F.: Thousand years of winter surface air temperature variations in Svalbard and
707 northern Norway reconstructed from ice-core data, Polar Res, 30, 7379,
708 https://doi.org/10.3402/polar.v30i0.7379, 2011.
709 Førland, E. J., Isaksen, K., Lutz, J., Hanssen-Bauer, I., Schuler, T. V., Dobler, A., Gjelten, H. M., and
710 Vikhamar-Schuler, D.: Measured and Modeled Historical Precipitation Trends for Svalbard, J
711 Hydrometeorol, 21, 1279–1296, https://doi.org/10.1175/JHM-D-19-0252.1, 2020.
712 Gabrielli, P., Barbante, C., Bertagna, G., Bertó, M., Binder, D., Carton, A., Carturan, L., Cazorzi, F.,
713 Cozzi, G., Dalla Fontana, G., Davis, M., De Blasi, F., Dinale, R., Dragà, G., Dreossi, G., Festi,
714 D., Frezzotti, M., Gabrieli, J., Galos, S. P., Ginot, P., Heidenwolf, P., Jenk, T. M., Kehrwald, N.,
715 Kenny, D., Magand, O., Mair, V., Mikhalenko, V., Lin, P. N., Oeggl, K., Piffer, G., Rinaldi, M.,
716 Schotterer, U., Schwikowski, M., Seppi, R., Spolaor, A., Stenni, B., Tonidandel, D., Uglietti, C.,
717 Zagorodnov, V., Zanoner, T., and Zennaro, P.: Age of the Mt. Ortles ice cores, the Tyrolean
718 Iceman and glaciation of the highest summit of South Tyrol since the Northern Hemisphere
719 Climatic Optimum, Cryosphere, 10, 2779–2797, https://doi.org/10.5194/tc-10-2779-2016, 2016.
720 Geyman, E. C., J. J. van Pelt, W., Maloof, A. C., Aas, H. F., and Kohler, J.: Historical glacier change
721 on Svalbard predicts doubling of mass loss by 2100, Nature, 601, 374–379,
722 https://doi.org/10.1038/s41586-021-04314-4, 2022.
723 Goto-Azuma, K., S. Kohshima, T., Kameda, S., Takahashi, O., Watanabe, Y. F., and Hagen., and J.
724 O.: An ice-core chemistry record from Snøfjellafonna, northwestern Spitsbergen, Ann. Glaciol.,
725 21, 213–218, 1995.
726 Hersbach, H., Bell, B., Berrisford, P., Hirahara, S., Horányi, A., Muñoz-Sabater, J., Nicolas, J.,
727 Peubey, C., Radu, R., Schepers, D., Simmons, A., Soci, C., Abdalla, S., Abellan, X., Balsamo,
728 G., Bechtold, P., Biavati, G., Bidlot, J., Bonavita, M., Chiara, G., Dahlgren, P., Dee, D.,
729 Diamantakis, M., Dragani, R., Flemming, J., Forbes, R., Fuentes, M., Geer, A., Haimberger, L.,
730 Healy, S., Hogan, R. J., Hólm, E., Janisková, M., Keeley, S., Laloyaux, P., Lopez, P., Lupu, C.,
731 Radnoti, G., Rosnay, P., Rozum, I., Vamborg, F., Villaume, S., and Thépaut, J.: The ERA5 global
732 reanalysis, Quarterly Journal of the Royal Meteorological Society, 146, 1999–2049,
733 https://doi.org/10.1002/qj.3803, 2020.
734 Hoffmann, G., Ramirez, E., Taupin, J. D., Francou, B., Ribstein, P., Delmas, R., Dürr, H., Gallaire,
735 R., Simões, J., Schotterer, U., Stievenard, M., and Werner, M.: Coherent isotope history of
736 Andean ice cores over the last century, Geophys Res Lett, 30, 2002GL014870,
737 https://doi.org/10.1029/2002GL014870, 2003.
738 Isaksen, K., Nordli, Ø., Førland, E. J., Łupikasza, E., Eastwood, S., and Niedźwiedź, T.: Recent
739 warming on Spitsbergen—Influence of atmospheric circulation and sea ice cover, Journal of
740 Geophysical Research: Atmospheres, 121, 11, 911–913, 931,
741 https://doi.org/10.1002/2016JD025606, 2016.
742 Isaksen, K., Nordli, Ø., Ivanov, B., Køltzow, M. A. Ø., Aaboe, S., Gjelten, H. M., Mezghani, A.,
743 Eastwood, S., Førland, E., Benestad, R. E., Hanssen-Bauer, I., Bråkkan, R., Sviashchennikov,

P., Demin, V., Revina, A., and Karandasheva, T.: Exceptional warming over the Barents area, Sci Rep, 12, 9371, https://doi.org/10.1038/s41598-022-13568-5, 2022.
Isaksson, E., Hermanson, M., Hicks, S., Igarashi, M., Kamiyama, K., Moore, J., Motoyama, H., Muir, D., Pohjola, V., Vaikmäe, R., van de Wal, R. S. W., and Watanabe, O.: Ice cores from Svalbard– –useful archives of past climate and pollution history, Physics and Chemistry of the Earth, Parts A/B/C, 28, 1217–1228, https://doi.org/10.1016/j.pce.2003.08.053, 2003.
Isaksson, E., Kekonen, T., Moore, J., and Mulvaney, R.: The methanesulfonic acid (MSA) record in a Svalbard ice core, Ann. Glaciol., 42, 345–351, 2005.
Kohler, J.: Mass balance for glaciers near Ny-Ålesund [Data set]. Norwegian Polar Institute, 2013.
Lind, S., Ingvaldsen, R. B., and Furevik, T.: Arctic warming hotspot in the northern Barents Sea linked to declining sea-ice import, Nat Clim Chang, 8, 634–639, https://doi.org/10.1038/s41558-018-0205-y, 2018.
Matoba, S., Narita, H., Motoyama, H., Kamiyama, K., and Watanabe, O.: Ice core chemistry of Vestfonna Ice Cap in Svalbard, Norway, Journal of Geophysical Research: Atmospheres, 107, ACH 19-1-ACH 19-7, https://doi.org/10.1029/2002JD002205, 2002.
Maturilli, M., Herber, A., and König-Langlo, G.: Climatology and time series of surface meteorology in Ny-Ålesund, Svalbard, Earth Syst. Sci. Data, 5, 155–163, https://doi.org/10.5194/essd-5-155-2013, 2013.
Nuth, C., Schuler, T. V., Kohler, J., Altena, B., and Hagen, J. O.: Estimating the long-term calving flux of Kronebreen, Svalbard, from geodetic elevation changes and mass-balance modeling, Journal of Glaciology, 58, 119–133, https://doi.org/10.3189/2012JoG11J036, 2017.
Østby, T. I., Schuler, T. v, Hagen, J. O., Hock, R., Kohler, J., and Reijmer, C. H.: Diagnosing the decline in climatic mass balance of glaciers in Svalbard over 1957–2014, Cryosphere, 11, 191–215, https://doi.org/10.5194/tc-11-191-2017, 2017.
Peeters, B., Pedersen, Å. Ø., Loe, L. E., Isaksen, K., Veiberg, V., Stien, A., Kohler, J., Gallet, J.-C., Aanes, R., and Hansen, B. B.: Spatiotemporal patterns of rain-on-snow and basal ice in high Arctic Svalbard: detection of a climate-cryosphere regime shift, Environmental Research Letters, 14, 015002, https://doi.org/10.1088/1748-9326/aaefb3, 2019.
van Pelt, W. J. J., Kohler, J., Liston, G. E., Hagen, J. O., Luks, B., Reijmer, C. H., and Pohjola, V. A.: Multidecadal climate and seasonal snow conditions in Svalbard, J Geophys Res Earth Surf, 121, 2100–2117, https://doi.org/https://doi.org/10.1002/2016JF003999, 2016.
van Pelt, W., Pohjola, V., Pettersson, R., Marchenko, S., Kohler, J., Luks, B., Hagen, J. O., Schuler, T. V, Dunse, T., Noël, B., and Reijmer, C.: A long-term dataset of climatic mass balance, snow conditions, and runoff in Svalbard (1957–2018), Cryosphere, 13, 2259–2280, https://doi.org/10.5194/tc-13-2259-2019, 2019.
Pohjola, V. A., Moore, J. C., Isaksson, E., Jauhiainen, T., Van de Wal, R. S. W., Martma, T., Meijer, H. A. J., and Vaikmäe, R.: Effect of periodic melting on geochemical and isotopic signals in an ice core from Lomonosovfonna, Svalbard, J. Geophys. Res. Atmos., 107, 1–14, 2002.
Rantanen, M., Karpechko, A. Yu., Lipponen, A., Nordling, K., Hyvärinen, O., Ruosteenoja, K., Vihma, T., and Laaksonen, A.: The Arctic has warmed nearly four times faster than the globe since 1979, Commun Earth Environ, 3, 168, https://doi.org/10.1038/s43247-022-00498-3, 2022a.
Rantanen, M., Karpechko, A. Yu., Lipponen, A., Nordling, K., Hyvärinen, O., Ruosteenoja, K., Vihma, T., and Laaksonen, A.: The Arctic has warmed nearly four times faster than the globe since 1979, Commun Earth Environ, 3, 168, https://doi.org/10.1038/s43247-022-00498-3, 2022b.
Ruppel, M. M., Soares, J., Gallet, J.-C., Isaksson, E., Martma, T., Svensson, J., Kohler, J., Pedersen, C. A., Manninen, S., Korhola, A., and Ström, J.: Do contemporary (1980–2015) emissions determine the elemental carbon deposition trend at Holtedahlfonna glacier, Svalbard?, Atmos Chem Phys, 17, 12779–12795, https://doi.org/10.5194/acp-17-12779-2017, 2017.

Salzano, R., Cerrato, R., Scoto, F., Spolaor, A., Valentini, E., Salvadore, M., Esposito, G., Sapio, S., Taramelli, A., and Salvatori, R.: Detection of Winter Heat Wave Impact on Surface Runoff in a Periglacial Environment (Ny-Ålesund, Svalbard), Remote Sens (Basel), 15, 4435, https://doi.org/10.3390/rs15184435, 2023.

Schuler, T. v, Kohler, J., Elagina, N., Hagen, J. O. M., Hodson, A. J., Jania, J. A., Kääb, A. M., Luks, B., Małecki, J., Moholdt, G., Pohjola, V. A., Sobota, I., and van Pelt, W. J. J.: Reconciling Svalbard Glacier Mass Balance, Front Earth Sci (Lausanne), 8, 2020.

Schwikowski, M., Döscher, A., Gäggeler, H. W., and Schotterer, U.: Anthropogenic versus natural sources of atmospheric sulphate from an Alpine ice core, Tellus B: Chemical and Physical Meteorology, 51, 938, https://doi.org/10.3402/tellusb.v51i5.16506, 1999.

Schyberg, H. , Yang, X. , Koltzow, M. , Amstrup, B. , ., Bakketun, B., Bazile, E. , Bojarova, J. , Box, J. , Dahlgren, P. , Hagelin, S. , Homleid, M. , Horanyi, A. , Hoyer, J. , Johansson, K. M. , Kornich, H. , le Moigne, P. , Lindskog, M. , Manninen, T. , Nielsen Englyst, P. , and and Wang, Z.: Arctic regional reanalysis on single levels from 1991 to present, , 2020.

Scoto, F., Sadatzki, H., Maffezzoli, N., Barbante, C., Gagliardi, A., Varin, C., Vallelonga, P., Gkinis, V., Dahl-Jensen, D., Kjær, H. A., Burgay, F., Saiz-Lopez, A., Stein, R., and Spolaor, A.: Sea ice fluctuations in the Baffin Bay and the Labrador Sea during glacial abrupt climate changes, Proceedings of the National Academy of Sciences, 119, e2203468119, https://doi.org/10.1073/pnas.2203468119, 2022.

Sigl, M., McConnell, J. R., Toohey, M., Curran, M., Das, S. B., Edwards, R., Isaksson, E., Kawamura, K., Kipfstuhl, S., Kruger, K., Layman, L., Maselli, O. J., Motizuki, Y., Motoyama, H., Pasteris, D. R., and Severi, M.: Insights from Antarctica on volcanic forcing during the Common Era, Nature Clim. Change, 4, 693–697, https://doi.org/10.1038/nclimate2293 http://www.nature.com/nclimate/journal/v4/n8/abs/nclimate2293.html#supplementary-information, 2014.

Sobota, I., Weckwerth, P., and Grajewski, T.: Rain-On-Snow (ROS) events and their relations to snowpack and ice layer changes on small glaciers in Svalbard, the high Arctic, J Hydrol (Amst), 590, 125279, https://doi.org/https://doi.org/10.1016/j.jhydrol.2020.125279, 2020.

Spolaor, A., Gabrieli, J., Martma, T., Kohler, J., Björkman, M. B., Isaksson, E., Varin, C., Vallelonga, P., Plane, J. M. C., and Barbante, C.: Sea ice dynamics influence halogen deposition to Svalbard, Cryosphere, 7, 1645–1658, https://doi.org/10.5194/tc-7-1645-2013, 2013a.

Spolaor, A., Gabrieli, J., Martma, T., Kohler, J., Björkman, M. B., Isaksson, E., Varin, C., Vallelonga, P., Plane, J. M. C., and Barbante, C.: Sea ice dynamics influence halogen deposition to Svalbard, Cryosphere, 7, 1645–1658, https://doi.org/10.5194/tc-7-1645-2013, 2013b.

Spolaor, A., Varin, C., Pedeli, X., Christille, J. M., Kirchgeorg, T., Giardi, F., Cappelletti, D., Turetta, C., Cairns, W. R. L., Gambaro, A., Bernagozzi, A., Gallet, J. C., Björkman, M. P., and Barbaro, E.: Source, timing and dynamics of ionic species mobility in the Svalbard annual snowpack, Science of The Total Environment, 751, 141640, https://doi.org/https://doi.org/10.1016/j.scitotenv.2020.141640, 2021.

Steffensen, J. P., Andersen, K. K., Bigler, M., Clausen, H. B., Dahl-Jensen, D., Fischer, H., Goto-Azuma, K., Hansson, M., Johnsen, S. J., Jouzel, J., Masson-Delmotte, V., Popp, T., Rasmussen, S. O., Röthlisberger, R., Ruth, U., Stauffer, B., Siggaard-Andersen, M.-L., Sveinbjörnsdóttir, Á. E., Svensson, A., and White, J. W. C.: High-Resolution Greenland Ice Core Data Show Abrupt Climate Change Happens in Few Years, Science (1979), 321, 680–684, 2008.

Steffensen Schmidt, L., Schuler, T. V, Thomas, E. E., and Westermann, S.: Meltwater runoff and glacier mass balance in the high Arctic: 1991–2022 simulations for Svalbard, EGUsphere, 2023, 1–32, https://doi.org/10.5194/egusphere-2022-1409, 2023.

Stenni, B., Curran, M. A. J., Abram, N. J., Orsi, A., Goursaud, S., Masson-Delmotte, V., Neukom, R., Goosse, H., Divine, D., van Ommen, T., Steig, E. J., Dixon, D. A., Thomas, E. R., Bertler, N. A. N., Isaksson, E., Ekaykin, A., Werner, M., and Frezzotti, M.: Antarctic climate variability

on regional and continental scales over the last 2000 years, Clim. Past, 13, 1609–1634, https://doi.org/10.5194/cp-13-1609-2017, 2017.
Thompson, L. G., Yao, T., Davis, M. E., Mosley-Thompson, E., Wu, G., Porter, S. E., Xu, B., Lin, P.-N., Wang, N., Beaudon, E., Duan, K., Sierra-Hernández, M. R., and Kenny, D. v.: Ice core records of climate variability on the Third Pole with emphasis on the Guliya ice cap, western Kunlun Mountains, Quat Sci Rev, 188, 1–14, https://doi.org/10.1016/j.quascirev.2018.03.003, 2018.
Thompson, L. G., Davis, M. E., Mosley-Thompson, E., Porter, S. E., Corrales, G. V., Shuman, C. A., and Tucker, C. J.: The impacts of warming on rapidly retreating high-altitude, low-latitude glaciers and ice core-derived climate records, Glob Planet Change, 203, 103538, https://doi.org/10.1016/j.gloplacha.2021.103538, 2021.
Vecchiato, M., Gambaro, A., Kehrwald, N. M., Ginot, P., Kutuzov, S., Mikhalenko, V., and Barbante, C.: The Great Acceleration of fragrances and PAHs archived in an ice core from Elbrus, Caucasus, Sci Rep, 10, 10661, https://doi.org/10.1038/s41598-020-67642-x, 2020.
Wendl, I. A., Eichler, A., Isaksson, E., Martma, T., and Schwikowski, M.: 800-year ice-core record of nitrogen deposition in Svalbard linked to ocean productivity and biogenic emissions, Atmos. Chem. Phys., 15, 7287–7300, https://doi.org/10.5194/acp-15-7287-2015, 2015.
Westermann, S., Ingeman-Nielsen, T., Scheer, J., Aalstad, K., Aga, J., Chaudhary, N., Etzelmüller, B., Filhol, S., Kääb, A., Renette, C., Schmidt, L. S., Schuler, T. V., Zweigel, R. B., Martin, L., Morard, S., Ben-Asher, M., Angelopoulos, M., Boike, J., Groenke, B., Miesner, F., Nitzbon, J., Overduin, P., Stuenzi, S. M., and Langer, M.: The CryoGrid community model (version 1.0) – a multi-physics toolbox for climate-driven simulations in the terrestrial cryosphere, Geosci Model Dev, 16, 2607–2647, https://doi.org/10.5194/gmd-16-2607-2023, 2023.
Wickström, S., Jonassen, M. O., Cassano, J. J., and Vihma, T.: Present Temperature, Precipitation, and Rain-on-Snow Climate in Svalbard, Journal of Geophysical Research: Atmospheres, 125, e2019JD032155, https://doi.org/https://doi.org/10.1029/2019JD032155, 2020.
Wolff, E. W., Barbante, C., Becagli, S., Bigler, M., Boutron, C. F., Castellano, E., de Angelis, M., Federer, U., Fischer, H., and Fundel, F.: Changes in environment over the last 800,000 years from chemical analysis of the EPICA Dome C ice core, Quaternary Sci Rev, 29, 285–295, 2010.
Zdanowicz, C. M., Proemse, B. C., Edwards, R., Feiteng, W., Hogan, C. M., Kinnard, C., and Fisher, D.: Historical black carbon deposition in the Canadian High Arctic: a >250-year long ice-core record from Devon Island, Atmos Chem Phys, 18, 12345–12361, https://doi.org/10.5194/acp-18-12345-2018, 2018.